Capacity and Error Probability Analysis of Neuro-Spike Communication Exploiting Temporal Modulation

Article *in* IEEE Transactions on Communications · December 2019

DOI: 10.1109/TCOMM.2019.2962805

3 authors:

Keyvan Aghababaiyan
University of Tehran
18 PUBLICATIONS **225** CITATIONS
SEE PROFILE

Vahid Shah-Mansouri
University of Tehran
96 PUBLICATIONS **1,250** CITATIONS
SEE PROFILE

Behrouz Maham
Nazarbayev University
156 PUBLICATIONS **2,321** CITATIONS
SEE PROFILE

Capacity and Error Probability Analysis of Neuro-Spike Communication Exploiting Temporal Modulation

Keyvan Aghababaiyan, *Student Member, IEEE*, Vahid Shah-Mansouri, *Member, IEEE*, and Behrouz Maham, *Senior Member, IEEE*

***Abstract*— In this paper, we consider a neuro-spike communication system between two neurons where nano-machines are used to enhance ability of neurons. Nano-machines can be employed for stimulation tasks when neurons have lost their ability to communicate. In the assumed system, information is conveyed via the time intervals between the input spikes train. For efficiency evaluation of temporal coding, we model the neuro-spike communication system by an additive Gamma noise channel. We present this model by considering different time distortion factors in the neuro-spike system. Then, we derive upper and lower bounds on the channel capacity. We analyze the channel capacity bounds as functions of the time intervals between the input spikes and the firing threshold of the target neuron. Moreover, we propose maximum likelihood and maximum a posteriori receivers and derive the resulting bit error probability when the system uses binary modulation. In addition, we obtain an upper bound for this error probability. Then, we extend this upper bound to the symbol error probability of the T-ary modulations. Simulation results show that this upper bound is tight. The derived results show that temporal coding has a higher efficiency than spike rate coding in terms of achievable data rate.**

***Index Terms*— Neuro-spike communication, temporal modulation, capacity bounds, symbol error probability, gamma distribution.**

I. Introduction

RECENT developments in nano-technology and communication engineering are expected to lead to a new generation of nano-scale devices implantable inside the human body [2], [3]. Nano-scale devices or nano-machines are capable of carrying out complex tasks and overcoming their individual limitations through interconnecting in a nano-network [4], [5]. Recently, intra-body nano-networks have been proposed for monitoring the nervous system [6]–[8]. The main goal of such system is to assist the development of new medical diagnosis and treatment techniques. A class of applications is based on the deployment of autonomous or coordinated nano-machines in the neuronal tissue, to directly apply or indirectly induce a stimulus [9]. The neuron is a biological computational unit with pre-synaptic input terminals, processing unit and post-synaptic output terminals [10]. Following this application, nano-machine to neuron interfaces can be used in the pre-synaptic and post-synaptic terminals.

The nervous system is a natural communication system in the body that conveys biological information. There are about 100 billion nerve cells in the human nervous system, and on average, each of them communicates directly with 1000 others [11]. The communication among neurons is called neuro-spike communication. Neuro-spike communication is a hybrid system comprising three main parts. In the first part, i.e., the axonal transmission, action potentials propagate along the nerve fiber, called axon. Note that an action potential is an oscillation of roughly 100 mV in the electrical potential across the cell velum that lasts for about 1 ms. Neuroscientists often refer to action potentials as *spike*. Since the spikes in the nervous system are similar, the information has to be encoded in the configurations of the spikes which propagate along the axon. *Neural coding* refers to the mapping from the stimulus to the configurations of the generated spikes by neurons [12]. In particular, neurons employ the spike rate and temporal coding to transmit information via action potentials. When a spike arrives at the end of the axon, the pre-synaptic terminals release packet of neuro-transmitters into the synaptic cleft between two adjoining neurons. The synaptic transmission, the second part of neuro-spike communication, begins with the releasing these packets. Every packet includes many neuro-transmitter molecules. Each neuro-transmitter propagates towards the receiving neuron via free diffusion. There are many post-synaptic terminals at the dendrites, where receptors are located which receive the propagated molecules. When a sufficient number of neuro-transmitters is absorbed, the final part of neuro-spike communication, called spike generation, is commenced due to the movement of ions. There is a population of ion channels at membrane of the output neuron. Thus, moving ions excites its membrane potential, and leads to the generation of a new action potential with firing of the neuron [12]. There is a threshold for each neuron that has to be excluded for firing. Thus, in the nervous system,

Manuscript received March 30, 2019; revised July 12, 2019 and November 5, 2019; accepted December 10, 2019. Date of publication December 27, 2019; date of current version April 16, 2020. This article was presented in part at the 2018 IEEE Wireless Communications and Networking Conference (WCNC 2018) [1]. The associate editor coordinating the review of this article and approving it for publication was M. Pierobon. *(Corresponding author: Vahid Shah-Mansouri.)*

Keyvan Aghababaiyan and Vahid Shah-Mansouri are with the School of Electrical and Computer Engineering, College of Engineering, University of Tehran, Tehran 14395-515, Iran (e-mail: aghababaiyan@ut.ac.ir; vmansouri@ut.ac.ir).

Behrouz Maham is with the Department of Electrical and Computer Engineering, School of Engineering, Nazarbayev University, Astana 010000, Kazakhstan (e-mail: behrouz.maham@nu.edu.kz).

Color versions of one or more of the figures in this article are available online at http://ieeexplore.ieee.org.

Digital Object Identifier 10.1109/TCOMM.2019.2962805

the information is transmitted from one neuron to another one by spikes.

In the nervous system, if spikes propagate from the pre-synaptic neuron to the post-synaptic neuron with a constant delay, when information is encoded by patterns of input spikes, the communication channel is *noiseless* and the output spikes pattern is identical to the input spikes pattern. However, this is not a realistic assumption in practice since there are many reasons which distort time of spikes in the neuro-spike communication system. We describe these reasons in different parts of neuro-spike communication in the following.

- *Axonal Transmission:* The traveling speed of the spikes along the axon is not constant. Lass and Abeles [13] found jitter in the speed of the spikes propagating through a single fiber of the frog sciatic nerve, to which a pair of stimuli was applied to generate a pair of output spikes. Moreover, the speed of a spike depends on the history of the spike train since the transmission of a spike modifies the physiological state of the axon. If a spike is generated before the original physiological state of the axon is restored, the traveling speed through the axon is affected [14].
- *Synaptic Transmission:* A spike is generated by the output neuron due to the integration of stimuli arriving at several different synapses associated with this neuron [15]. Since diffusion of neuro-transmitters in the synapse is random, integrated stimuli reach the firing threshold randomly. Moreover, size of released neuro-transmitter vesicles to the synaptic cleft due to arriving a spike is random [16].
- *Spike Generation:* The amplitude of the post-synaptic responses is different trial-to-trial [17]. Thus, the stimuli of different vesicles for spike generation are not similar. Moreover, when the integrated stimuli approaches the threshold value, whether an output spike occurs or not is fully stochastic [18]. This means, sometimes an output spike is generated and sometimes it is not [19].

For these reasons, generated spikes travel at different speeds and the time intervals between them are altered as they propagate between two neurons. In temporal modulation, the time intervals between input spikes are important and the input spike pattern represents the information that is encoded. The stochastic properties of neuro-spike communication channel impair the time relations between input spikes. This phenomenon is referred to as channel noise. Channel noise affects the action potential propagation time and produces trial-to-trial variability in action potential timing.

Neuro-spike communication has been the focus of recent researches. It has been shown in [12] that the efficiency of neuro-spike communication is acceptable in terms of robustness, speed, and reliability. In [20], a mathematical model has been provided which shows how a neuron stochastically processes data and transmits information. A physical channel representation has been proposed in [17] to characterize the fundamental properties of neuro-spike communication. This model has been inspired by the neuro-spike communication in the Cornu Ammonis (CA) region, a specific zone in the hippo-campus area of the brain. An alternative model for the neuron-to-neuron communication process has been proposed in [21]. In [22], a mathematical channel model for synaptic communication via modeling the diffusion and binding of neuro-transmitters and reabsorption of neuro-transmitters by the transmitting neuron has been proposed. The authors of [23] have proposed a realistic pool-based model for vesicle release and have evaluated the capacity of information transmission for this process. The authors of [24] have derived theoretical upper bounds on the capacity of both bipartite and tripartite synapses. The authors of [16] have investigated the multiple-access communications among neurons. In [25] and [26], we have derived the axonal transmission channel capacity by modeling the input spike train and the axonal noise. In [27], [28] and [29], the effect of axonal variability on the synaptic transmission has been studied. However, none of the above works have considered the temporal modulation employing spike intervals for information transfer in neuro-spike communication. In this paper, we study the neuro-spike communication timing channels and their capacity bounds. We consider a neuro-spike communication channel between two neurons located in the motor cortex region of the brain where the information is encoded by spike time intervals [30]. We take into account the variations in propagation time in the axonal pathway, synaptic transmission, and spike generation parts. In particular, for synaptic transmission, we consider the Brownian motion model which is a commonly used model for the propagation of neuro-transmitters in the synaptic cleft. In this paper, we assume transmitter and receiver are ideal and do not include errors. Hence, in our model, the communication is corrupted by the randomness originating from the variations of the propagation time of spikes. The key contributions of this paper can be summarized as follows:

- We model the jitter of the neuro-spike communication channel between two neurons, located in the motor cortex region exploiting temporal modulation, as channel noise. We show a Gamma random variable is suitable to model this jitter. Thus, the neuro-spike communication channel is modeled as communication over an additive Gamma noise channel.
- Exploiting the additive Gamma noise model, we develop upper and lower bounds on the capacity of the considered neuro-spike communication system. We derive these bounds by using the additivity property of Gamma distributions.
- We investigate the receiver design for neuro-spike communication systems exploiting temporal modulation and present ML and MAP detectors for binary modulation. Moreover, we derive bit error probability and an upper bound on the corresponding bit error probability of ML detector.
- We extend the ML detector to T-ary modulation, and derive an upper bound on the corresponding symbol error probability.

This paper is organized as follows. In Section II, we present the system model for neuro-spike communication when temporal modulation is used. This system model is exploited in Section III to derive capacity bounds for the neuro-spike

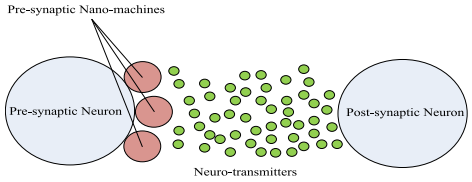

(a) Pre-synaptic neuron is unhealthy.

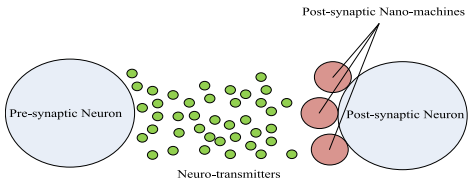

(b) Post-synaptic neuron is unhealthy.

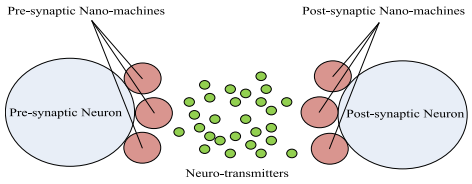

(c) Both of neurons are unhealthy.

Fig. 1. Employing nano-machines for stimulation tasks when neurons have lost their ability to communicate.

communication channel. In Section IV, we develop a Maximum Likelihood Estimator (MLE) for the transmission time of spikes. In addition, we design ML and MAP detectors for temporal modulations. Furthermore, we analyze the error probability of different modulation formats in this section. Finally, in Section V, we conclude this paper.

II. System Model

Neuro-degenerative diseases are incurable and debilitating conditions that result in progressive degeneration or death of nerve cells. In these situations, the connection of neurons is lost. Recent experiments have shown a loss of neurons connectivities increases average path-length between neurons. This is the main reason of Alzheimer's disease [31]. The neurons size ranges from 4 to $100\,\mu$m which appears extremely small; however, from the molecular point of view, there is enough space to place nano-scale devices. These nano-machines are employed to reconnect the nerve cells. There are three scenarios as shown in Fig. 1. In these scenarios, one or more nano-machines connect to the unhealthy neurons. When the pre-synaptic neuron is unhealthy, pre-synaptic nano-machines release neuro-transmitters to the synaptic cleft according to the received stimuli from the pre-synaptic neuron as shown in Fig. 1 (a). When the post-synaptic neuron is unhealthy, post-synaptic nano-machines bind neuro-transmitters from the synaptic cleft and stimulate the post-synaptic neuron as shown in Fig. 1 (b). The third scenario is synthesis of the first and second scenarios as shown in Fig. 1 (c). The connection between nano-machines and neuron is called gap junction [9]. In the gap junctions, the membranes of neuron and nano-machines are in direct contact where they are separated by only $3\,$nm. In every side of this connection, clusters of connexine (Cx36) proteins [32] are combined to form a channel with diameter $1-2\,$nm. The connexine allows bidirectional flows of ions between neuron and nano-machines. Passing the flows of ions between neuron and nano-machines through the gap junction is fast and it takes a short time in comparison to the time required for diffusion of neuro-transmitters across the synaptic cleft. Hence, neglecting the effect of gap junctions, the system model of neuro-spike communication comprises three main parts, i.e., the axonal pathway, synaptic transmission, and spike generation. We investigate these parts in detail to develop a suitable mathematical model for the neuro-spike communication jitter. In neuro-spike communication systems, jitter is referred to the variation in the delay of the spikes. Since we assume the communicating neurons are located in the motor cortex region, we consider the neurons of this region for our model. The motor cortex is a region in the cerebral cortex involved in the planning, control, and execution of voluntary movements.

A. Variation of Propagation Time Along the Axonal Pathway

In the axonal pathway, due to the refractory period, the pattern of output spike train is different from the pattern of input spikes. The refractory period cuts off short action potential intervals and alters the propagation velocities of the spikes. Hence, the biological information which is encoded by the time intervals between the spikes and the instantaneous spike rate is impaired. Exploiting biophysical theory and stochastic simulations have demonstrated that there is a significant variation in the action potential propagation time along axons with different diameters [33], [34]. The variability in the post-axonal responses will increase in the longer and thinner axons. The authors of [33] have studied the movement of triggered action potentials along the axons of Intra Telencephalic (IT) and Pyramidal Track (PT) neurons in the motor cortex region. They have reported a short latency and a temporal variation in the propagation time of the action potentials. According to the results reported in [33] (Figs. 3 (c), (g) and Fig. 5 (g)), a Gaussian distribution is a suitable model to describe the variation of the action penitential propagation time along the axon. For modeling the propagation time in the axonal pathway, we assume the length of the axon is d_a and the average velocity of propagation of spikes along the axon is $\bar{V}$. We adopt a Gaussian stochastic variable to model the transmission time of the spikes along the axon, i.e., $t_a \sim \mathbb{N}(\mu_a, \sigma_a^2)$, and

$$f(t_a) = \frac{1}{\sqrt{2\pi\sigma_a^2}} e^{-\frac{(t_a-\mu_a)^2}{2\sigma_a^2}}, \tag{1}$$

where $\mu_a = \frac{\bar{V}}{d_a}$ is the mean of the traveling time and its variance is σ_a^2.

B. Synaptic Transmission Model

In this paper, we consider chemical synapses which are specialized junctions where cells of the nervous system communicate with one another. In the synaptic transmission part,

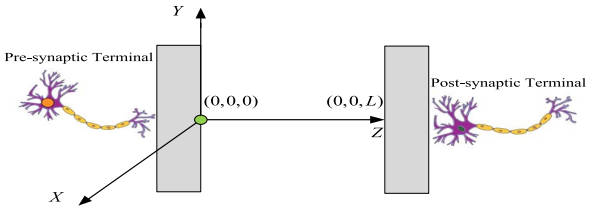

Fig. 2. The diffusion process of neuro-transmitters in the synaptic cleft with considering spillover effect.

we assume that when a spike arrives at the pre-synaptic terminal, the content of one vesicle of excitatory neuro-transmitters is released. The release of neuro-transmitters influences the membrane ion flow of the output neuron to increase the probability that the cell will produce an action potential, i.e., it has an excitatory effect. We consider Glutamate as the neuro-transmitters. Glutamate is used by the great majority of fast excitatory synapses in the brain [35]. We assume each vesicle contains N_{Glu} neuro-transmitters. The vesicle release is very fast and it takes a short time for all of the neuro-transmitters to enter the cleft compared to the time required for diffusion across the cleft. Hence, we assume that the neuro-transmitters are released instantaneously.

Moreover, we take into account that the movement of neuro-transmitter molecules is governed by a Brownian motion [36]. Hence, the neuro-transmitters concentration in different locations and for different times can be approximated by Fick's equation [37] as

$$\frac{\partial C(x,y,z,t)}{\partial t} = D\nabla^2 C(x,y,z,t), \tag{2}$$

where D is the diffusion coefficient, $t \geq 0$, and $(x,y,z) \in \Re^2 \times [0,L]$ according to Fig. 2. Since the content of vesicle is released instantaneously and we assume that the release befalls at the origin of x-y plane, the initial distribution for concentration of neuro-transmitters is described as

$$C(x,y,z,0) = N_{\text{Glu}}\delta(x,y,z), \tag{3}$$

where N_{Glu} is the number of neuro-transmitters in a vesicle. Next, we assume that there is no flux of neuro-transmitters through pre-synaptic and post-synaptic membranes. It results the boundary conditions as

$$\frac{\delta}{\delta z}C(x,y,0,t) = \frac{\delta}{\delta z}C(x,y,L,t) = 0. \tag{4}$$

Recent studies showed that neuro-transmitters which are released at synapses, sometimes diffuse long enough distances to activate receptors located outside the synaptic cleft or even in neighboring synapses. This phenomenon is termed *spillover* which has significant physiological effects on the synaptic transmission [38]. Considering the effect of spillover, the solution of the diffusion equation in terms of Fourier Series in a domain between two parallel planes with infinite extent is obtained as [39]

$$C(x,y,z,t) = \frac{N^t_{\text{Glu}}}{4\pi LDt}\exp(-\frac{x^2+y^2}{4Dt}) \left(1 + 2\sum_{n=1}^{N}\cos\Big(\frac{n\pi z}{L}\Big)\exp\left(-\frac{(n\pi)^2 Dt}{L^2}\right)\right), \tag{5}$$

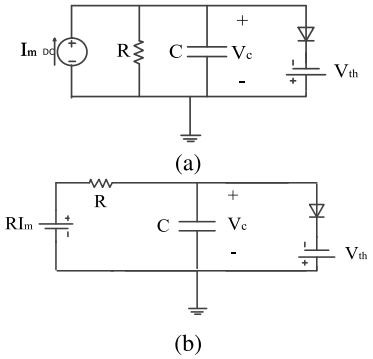

Fig. 3. (a) Integrate-and-Fire (I&F) system model. (b) The equivalent model by employing Thévenin's theorem.

where N is the number of Fourier modes taken in the approximation and N^t_{Glu} is the number of Glutamate molecules in the synapse at time t. It is obtained by subtracting the number of bound neuro-transmitters from N_{Glu}, i.e., $N^t_{\text{Glu}} = N_{\text{Glu}} - \sum_{t'=0}^{t^-} \hat{N}^{t'}_{\text{Glu}}$. Bound neuro-transmitters are counted from the moment of releasing vesicle up to time t^-.

A fraction of the neuro-transmitters are reabsorbed by the pre-synaptic terminal for recycling. Therefore, we consider the impact of this reuptake process to obtain a more realistic model. To model the reuptake process, we consider the same concentration as in no-flux case with modifying the coefficient of Fourier modes based on the uptake probability, i.e., P_u. When the reuptake probability is 0, i.e., $P_u = 0$, no neuro-transmitter which hits the pre-synaptic boundaries is absorbed. On the other hand, when the reuptake probability tends to 1, i.e., $P_u = 1$, all particles are absorbed. Hence, through considering the corresponding modification to reuptake process, the neuro-transmitters concentration is obtained as

$$C(x,y,z,t) = \frac{N^t_{\text{Glu}}}{4\pi LDt}\exp(-\frac{x^2+y^2}{4Dt}) \left(1 + 2\sum_{n=1}^{N}(1-P_u)^n\cos\Big(\frac{n\pi z}{L}\Big)\exp\left(-\frac{(n\pi)^2 Dt}{L^2}\right)\right). \tag{6}$$

C. Spike Generation

We consider an efficient model for generation of spikes, which is referred to as Integrate-and-Fire (I&F) model [40] as shown in Fig. 3 (a). In this model, the neuron is modeled as a capacitor, C. There is a threshold voltage for neurons and they can generate a spike when their membrane voltage exceeds this threshold voltage. According to Fig. 3 (a), we have

$$I_m(t) = \frac{V_c(t)}{R} + C\frac{dV_c(t)}{dt}, \tag{7}$$

where $V_c(t)$ is the voltage of capacitor C, R is the value of the neuron membrane resistance, and $I_m(t)$ is the current that results from movement of ions across the neuron membrane. By employing the Thévenin's theorem, the described model

in Fig. 3 (a) can be replaced by the model in Fig. 3 (b). Thus, the expression in (7) is converted to

$$V_m(t) = V_c(t) + \tau_m \frac{dV_c(t)}{dt}, \tag{8}$$

where $V_m(t) = RI_m(t)$ and $\tau_m = RC$ which is the time constant of the RC circuit. In the I&F model, the excitatory neuro-transmitters make positive charge onto the capacitor through depolarization. Moreover, the voltage waveform generated at one receptor in response to a neuro-transmitter, i.e., Excitatory Post-Synaptic Potential (EPSP), can be modeled by an alpha function as [17]

$$h(t) = h_{\text{peak}} \frac{t}{\tau} \exp(1 - \frac{t}{\tau}) u(t), \tag{9}$$

where τ is a constant associated with the type of the receptor, h_{peak} is the peak EPSP magnitude, and $u(t)$ is the Heaviside step function which is defined as $u(t) = 1$ for $t \geq 0$ and $u(t) = 0$ for $t < 0$. We consider α-amino-3-hydroxy-5-methyl-4-isoxazolepropionic acid (AMPA) receptors for Glutamate neuro-transmitters. Moreover, it is assumed that neuro-transmitters are independent. We assume receptors bind neuro-transmitters in a small volume around them which is referred to as the effective volume [41]. The probability of finding each neuro-transmitter inside the effective volume around a receptor, i.e., V_e, at time t is obtained as

$$P_e{}^t = \int\limits_{V_e} \int \int C(x, y, z, t) dx dy dz. \tag{10}$$

Thus, the binding probability $P_e{}^t$ for an unoccupied receptor at time t can be described as $P^t_{\text{Glu}} = 1 - (1 - P^t_e)^{N^t_{\text{Glu}}}$, where N^t_{Glu} is the number of unbound excitatory neuro-transmitters in the synaptic cleft at time t with considering the reuptake process. Therefore, the number of received neuro-transmitters at time t can be derived as $\hat{N}^t_{\text{Glu}} = N^t_{\text{Glu}} P^t_{\text{Glu}}$. When we only consider the effect of one received neuro-transmitter, the generated voltage at the post-synaptic terminal becomes

$$\hat{V}_m(t) = h(t). \tag{11}$$

The Laplace transform of $\hat{V}_m(t)$ is given by

$$\hat{V}_m(s) = h_{\text{Peak}} \frac{e}{\tau \left(s + \frac{1}{\tau}\right)^2}. \tag{12}$$

Thus, according to the expression in (8), the Laplace transform of the voltage of the capacitor resulted from one neuro-transmitter, i.e., $\hat{V}_c(s)$ is obtained as

$$\hat{V}_c(s) \ = h_{\text{Peak}} \frac{e}{\tau \left(s + \frac{1}{\tau}\right)^2 (1 + \tau_m s)}. \tag{13}$$

Hence, the voltage of capacitor is derived as

$$\hat{V}_c(t) = h_{\text{Peak}} \left(\frac{\tau \tau_m^2 (e^{-\frac{t}{\tau_m}} - e^{-\frac{t}{\tau}})}{(\tau - \tau_m)^2} + \frac{\tau_m t e^{-\frac{t}{\tau}}}{(\tau - \tau_m)} \right) e. \tag{14}$$

Next, by considering the effect of all bound neuro-transmitters at time t, i.e., $\hat{N}^t_{Glu}$, the voltage of capacitor is derived as

$$V_c(t) = \hat{N}^t_{Glu} \hat{V}_c(t) + V_c(0), \tag{15}$$

TABLE I
SIMULATION PARAMETERS

Parameter	Symbol	Value
Neuro-transmitters in a Vesicle	N_{Glu}	Random $(2000 - 4000)$ [42]
Synaptic cleft width	L	20 nm [43]
Diffusion coefficient	D	$0.1\ \mu\text{m}^2/\text{ms}$ [44]
Number of receptors	M	100 [45]
Effective Volume	V_e	$0.5\,\text{nm} \times 0.5\,\text{nm} \times 0.5\,\text{nm}$
Reuptake Probability	P_u	0.1
I&F model time constant	τ_m	10 ms
Time reaches peak for EPSP	τ	1 ms [46]
Mean latency of axon	t_a	5 ms [33]
Variance of latency of axon	σ_a	0.5 ms [33]
Voltage threshold	V_{th}	-55 mV
Initial voltage of C	$V_c(0)$	-70 mV
Peak magnitude of the EPSP	h_{peak}	$400\ \mu$V [47]
Number of Fourier modes	N	5

where $V_c(0)$ is the initial voltage of C. In our model, we assume spikes are generated whenever the voltage $V_c(t)$ exceeds a voltage threshold, i.e., V_{th}. Then, the diode momentarily turned on to generate a spike. We define the time of spike generation as $t_d = t_x + t_a$, where t_a is the propagation time along the axon and t_x is the time that the voltage $V_c(t)$ reaches to the threshold value, i.e., V_{th}. This means $t_x = \{t \in \Re \,|V_c(t) = V_{th}\}$. Next, we analyze $f(t_d)$ by numerical methods and since it cannot be described in a closed form, we endeavor to approximate $f(t_d)$ by known distributions.

We perform Monte Carlo simulation to analyze the $f(t_d)$ with parameters given in Table I. Fig. 4 (a)-(c) show the $f(t_d)$ in this scenario. It can be observed that PDF of t_d is generally skewed toward higher delays. Hence, Gamma, Inverse Gaussian and Log-Normal distributions plus a constant value can be suitable candidates to approximate the $f(t_d)$. These distributions have different parameters for fitting to the $f(t_d)$. We summarize these distributions and their parameters in the following. All distributions have a constant shift for modeling the minimum value of t_d.

$$\mathbb{G}(\alpha, \beta, \Delta) = \frac{\beta^\alpha}{\Gamma(\alpha)} (x - \Delta)^{\alpha - 1} e^{-\beta(x - \Delta)},\ x > \Delta, \tag{16}$$

$$\mathbb{IG}(\mu, \lambda, \Delta) = \left(\frac{\lambda}{2\pi (x - \Delta)^3} \right)^{0.5} e^{-\frac{\lambda (x - \Delta - \mu)^2}{2\mu^2 (x - \Delta)}},\ x > \Delta, \tag{17}$$

$$\mathbb{LN}(\mu, \sigma^2, \Delta) = \frac{1}{(x - \Delta)\sigma\sqrt{2\pi}} e^{-\frac{(Ln(x - \Delta) - \mu)^2}{2\sigma^2}}, \quad x > \Delta. \tag{18}$$

Then, we compare these distributions in terms of Root Mean Square Error (RMSE) to find the best approximation for $f(t_d)$. The RMSE can be defined as

$$\int\limits_0^\infty (f(t_d) - f(P_1, P_2, \Delta))^2 dt_d, \tag{19}$$

where according to (16)-(18), (P_1, P_2) denote (α, β) in Gamma, (μ, λ) in Inverse Gaussian, and (μ, σ) in Log-Normal distribution and Δ is a constant shift. Tables II, III, and IV report the RMSE of the mentioned distributions for different values of their parameters. We highlight the optimum parameters of each distribution. It can be observed that Gamma distribution has a lower RMSE in comparison to other distributions. Hence, we conclude that the Gamma distribution

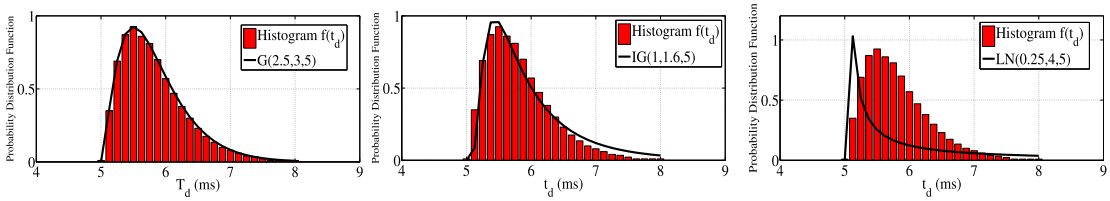

Fig. 4. (a) $f(t_d)$ and the best approximated Gamma distribution. (b) $f(t_d)$ and the best approximated Inverse Gaussian distribution. (c) $f(t_d)$ and the best approximated Log-Normal distribution.

TABLE II
THE RMSE OF THE APPROXIMATION OF $f(t_d)$ BY GAMMA DISTRIBUTIONS WITH DIFFERENT PARAMETERS

	β				
α	2.5	2.75	3	3.25	3.5
2	0.0630	0.0979	0.1375	0.1770	0.2152
2.25	0.0385	0.0302	0.0650	0.1053	0.1442
2.5	0.0881	0.0440	**0.0086**	0.0417	0.0807
2.75	0.1414	0.0995	0.0601	0.0286	0.0345
3	0.1898	0.1503	0.1127	0.0783	0.0517

is the best approximation for $f(t_d)$. Next, we choose the optimum parameters of the approximated Gamma distribution in different simulation scenarios by minimizing the RMSE as

$$(\alpha^*, \beta^*, \Delta^*) = \underset{\alpha,\beta,\Delta}{\operatorname{argmin}} \int_0^\infty \left(f(t_d) - \mathbb{G}(\alpha, \beta, \Delta)\right)^2 dt_d. \quad (20)$$

D. Modeling the Jitter of Neuro-Spike Communication Channel as Channel Noise

The output spikes arrival times are affected by different delays. When the propagation delay is constant, it is possible to obtain the input spike times according to the output arrival times; however, the spike propagation delays are fluctuated due to the neuro-spike communication channel jitter. We consider this jitter as an additive noise in the form of a random propagation delay. In this paper, we assume this jitter is the only source of uncertainty in output spikes arrival times. Since this noise has a Gamma distribution, we refer to the channel as an additive Gamma noise channel. Since the obtained Gamma distribution has a time shift from the origin, we consider the delay of the channel contains two terms. The minimum propagation delay, denoted as τ, which is deterministic and a random delay which is modeled by a Gamma distribution without any shift, referred to as N. Thus, the arrival time of the output spike at the post-synaptic neuron can be modeled as

$$Y' = X + N + \tau, \quad (21)$$

where X is the input spike time. For simplicity, since τ is a deterministic term, we define $Y = Y' - \tau$, and henceforth, we consider Y as the arrival time of the output spike. Moreover, we can consider N as a Gamma random variable with the following PDF:

$$f_N(n) = \frac{\beta^\alpha}{\Gamma(\alpha)} n^{\alpha-1} e^{-\beta n} = \mathbb{G}(\alpha, \beta). \quad (22)$$

By substituting the expression in (21) into (22) and considering the fact that $Y = Y' - \tau$, the conditional PDF of the arrival time of the output spike, i.e., $Y = y$ when the input spike is propagated at $X = x$ can be obtained as

$$f_{y|x}(y|x) = \begin{cases} \dfrac{\beta^\alpha}{\Gamma(\alpha)}(y-x)^{\alpha-1} e^{-\beta(y-x)}, & y > x, \\ 0, & y \le x. \end{cases} \quad (23)$$

III. CAPACITY BOUNDS OF NEURO-SPIKE COMMUNICATION CHANNEL

In this section, we analyze the capacity of the neuro-spike communication channel when we encode the information by the input spike train time intervals. According to the presented model in (21), the mutual information between the input X and the output Y of the neuro-spike communication channel is obtained by

$$I(X;Y) = h(Y) - h(Y|X) = h(Y) - h(X+N|X), \quad (24)$$

where $h(\cdot)$ is the entropy function. Since X and N are independent processes, we have

$$I(X;Y) = h(Y) - h(N|X) = h(Y) - h(N). \quad (25)$$

The capacity of a channel is defined as the maximum mutual information between its input and output which is optimized over all possible input distributions $f_X(x)$. The constraints on the input signal X determine the set of all possible input distributions. The constraints on the input signal are application dependent, e.g., both peak-constrained and mean constrained inputs can be considered based on the application. In this paper, we consider the mean constrained input signal since the average arrival time of input spikes is affected by the average input spike rate. Moreover, the peak constraints are not analytically tractable. Thus, we assume the transmitter neuron waits less than m seconds in average to transmit each input spike. Hence, the channel capacity with input X and mean constraint $\mathbb{E}[X] \le m$ is defined as

$$C = \max_{f_x(x):\mathbb{E}(X)\le m} I(X;Y). \quad (26)$$

The expected value of channel jitter noise, i.e., $\mathbb{E}(N)$ is finite. Thus, the expected value of arrival times of the output spikes at the receiver nano-machine is constrained, i.e., $\mathbb{E}(Y) = \mathbb{E}(X) + \mathbb{E}(N) \le m + \mathbb{E}(N)$. From this expression, we can conclude since the PDF of N is supported on $[0, \infty)$, the peak constraint is not meaningful for the arrival times at the receiver nano-machine. Unfortunately, there is no closed form

TABLE III
THE RMSE OF THE APPROXIMATION OF $f(t_d)$ BY INVERSE GAUSSIAN DISTRIBUTIONS WITH DIFFERENT PARAMETERS

	λ								
μ	1.3	1.4	1.5	1.6	1.7	1.8	1.9	2	2.1
0.9	0.0925	0.0851	0.0800	0.0772	0.0764	0.0774	0.0779	0.0836	0.0881
0.95	0.0839	0.0768	0.0723	0.0702	0.0703	0.0723	0.0758	0.0804	0.0857
1	0.0796	0.0734	0.0699	**0.0690**	0.0704	0.0734	0.0778	0.0831	0.0890
1.05	0.0787	0.0738	0.0718	0.0723	0.0747	0.0787	0.0838	0.0895	0.0958
1.1	0.0805	0.0771	0.0766	0.0782	0.0817	0.0863	0.0919	0.0980	0.1044
1.15	0.0840	0.0822	0.0829	0.0856	0.0898	0.0950	0.1009	0.1072	0.1138

TABLE IV
THE RMSE OF THE APPROXIMATION OF $f(t_d)$ BY LOG-NORMAL DISTRIBUTIONS WITH DIFFERENT PARAMETERS

	σ									
μ	0.5	0.75	1	1.25	1.5	1.75	2	2.25	2.5	3
0	0.444	0.401	0.359	0.347	0.343	0.341	0.340	0.340	0.340	0.340
0.25	0.432	0.369	0.351	0.350	0.347	0.343	**0.338**	0.338	0.338	0.338
0.5	0.398	0.361	0.371	0.368	0.358	0.348	0.342	0.338	0.338	0.338
0.75	0.412	0.395	0.387	0.374	0.367	0.353	0.345	0.339	0.339	0.339
1	0.427	0.409	0.396	0.389	0.371	0.356	0.349	0.340	0.340	0.340

solution for the channel capacity with Gamma distribution noise unlike the AWGN channel. Hence, we exploit Gamma distribution function to find upper and lower bounds on the channel capacity. Prior to obtain these bounds, we present two properties of the Gamma distribution function that we use them later on.

Property 1 (Differential entropy of Gamma distributions): We describe the differential entropy of a Gamma distribution by $h_{\mathbb{G}}(\cdot)$ based on parameters α and β as

$$h_{\mathbb{G}}(\alpha,\beta)=\alpha-\ln(\beta)+\ln(\Gamma(\alpha))+(1-\alpha)\,\Psi(\alpha), \quad (27)$$

where $\Psi(\alpha)=\frac{\Gamma'(\alpha)}{\Gamma(\alpha)}$ and $\Gamma(\alpha)=\int_0^\infty q^{\alpha-1}e^{-q}dq$. This differential entropy was proved in [1].

Property 2 (Additivity property of Gamma distributions): Assume $N_i\sim\mathbb{G}(\alpha_i,\beta),\ i=1,2,\ldots,L$ are not necessarily independent Gamma random variables. Then, $N=\sum_{i=1}^{L}N_i$ is a Gamma random variable as $N\sim\mathbb{G}\left(\sum_{i=1}^{L}\alpha_i,\beta\right)$. This property was proved in [1].

By using properties 1 and 2, the following theorem presents the capacity bounds of neuro-spike communication channel.

Theorem 1: The capacity of neuro-spike channel with additive Gamma noise, which is defined in (26), is bounded as

$$h_{\mathbb{G}}(\alpha+m\beta,\beta)-h_{\mathbb{G}}(\alpha,\beta)\le C\le\ln\left((m+\frac{\alpha}{\beta})e\right)-h_{\mathbb{G}}(\alpha,\beta), \quad (28)$$

where $h_{\mathbb{G}}(\alpha,\beta)$ is obtained by Property 1.

Proof: The proof is given in Appendix A.

Moreover, we consider a Doubly Poisson distribution to model the input spike train times. Since there may be numerous independent sources that produce the excitation, the input spike train can be assumed as a Poisson process. Moreover, the arrival of the stimuli can result no impulse, one impulse or more than one impulse independent of time; therefore, the firing rate of the neuron is itself a stochastic process as well. This type of Poisson process is called Doubly Poisson. In this scenario, we can only describe $f_Y(y)$ in a closed form. Thus, numerical methods is exploited to derive the mutual information. We assume $\lambda(t)$ is the intensity of Doubly Poisson process. The optimum distribution for $\lambda(t)$ is described as [25]

$$\lambda(t)=\begin{cases}\lambda, & P_1=P_\lambda,\\ 0, & P_0=1-P_\lambda.\end{cases} \quad (29)$$

Since the waiting times for Poisson distribution is an exponential distribution with parameter $\lambda(t)$, according to the expression in (29), the distribution of input spikes intervals is obtained as

$$f_X(x)=\begin{cases}\lambda e^{-\lambda x}u(x), & P_1=P_\lambda,\\ \delta(x-k), & P_0=1-P_\lambda,\end{cases} \quad (30)$$

where $k=\frac{m-P_\lambda\lambda}{1-P_\lambda}$ since we have $\mathrm{E}(x)=m$. Hence, according to the expressions in (22) and (30), the output distribution is derived by convolution of the input and channel noise distributions as

$$f_Y(y)=P_\lambda\left(\lambda e^{-\lambda y}u(y)\right)*\left(\frac{\beta^\alpha y^{\alpha-1}e^{-\beta y}}{\Gamma(\alpha)}u(y)\right)+(1-P_\lambda)\left(\frac{\beta^\alpha(y-k)^{\alpha-1}e^{-\beta(y-k)}}{\Gamma(\alpha)}u(y-k)\right), \quad (31)$$

where $*$ is the convolution operator.

Unlike AWGN channels, in our channel model, there is no parameter like SNR which determines the mutual information. In this condition, the mutual information is a function of both average input spike train intervals and the receiver threshold, i.e., V_{th}. Fig. 5 (a) shows the mutual information versus the average input spike train intervals by considering a Doubly Poisson distribution with $P_\lambda=0.5$ as distribution of the times of input spike train. Moreover, the upper and lower bounds of channel capacity are shown where the output distribution is considered as exponential and Gamma distributions in these scenarios, respectively. As can be observed, the upper and lower bounds are close to each others for shorter spike

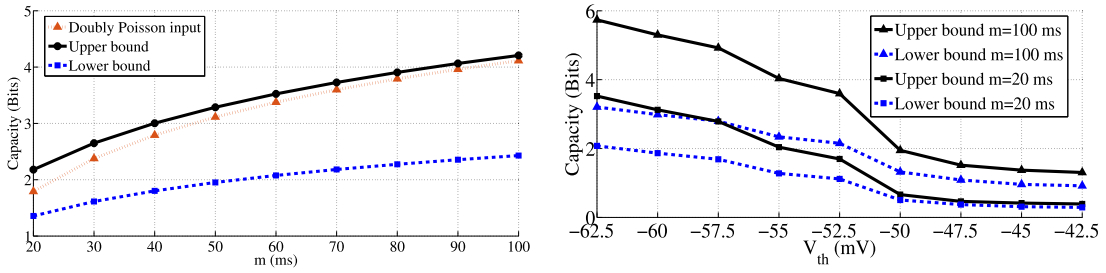

(a) (b)

Fig. 5. (a) The upper and lower bounds of the channel capacity versus different values of input spike train intervals for $V_{th} = -55\,\text{mV}$. (b) The upper and lower bounds of the channel capacity versus different values of V_{th}.

intervals. In addition, the input with Doubly Poisson distribution tracks the upper bound for different input intervals. To evaluate the performance of using temporal coding in neuro-spike communication systems, we compare the obtained results based on the proposed model with reported results in existing information-theoretic literature about nervous system. The upper and lower bounds on the capacity of neuro-spike communication system using spike rate coding have been presented in [48] for different spike frequencies. By comparison between the obtained results and Fig. 5 in [48], for the same spike frequencies, we conclude that temporal coding has a higher efficiency than spike rate coding in terms of achievable data rate. Moreover, Fig. 5 (b) shows the mutual information versus different values of V_{th}. It can be observed the upper and lower capacity bounds reduce when V_{th} increases since the jitter of channel increases in this situation.

IV. Receiver Design for Neuro-Spike Communication System With Temporal Modulations

In this section, we discuss the error probability of the neuro-spike channel by recovering the transmission time of input spikes from the arrival times of output spikes when we employ different modulations. First, we obtain MLE for the transmission time based on arrival time. Then, we develop the ML and MAP receivers and analyze the error probability for ML detector.

A. Maximum Likelihood Estimator

We denote the MLE of X as $\hat{X}_{ML}$, which is given by

$$\hat{X}_{ML} = \arg\max_{t} f_{Y|X}(Y|X=t), \tag{32}$$

where

$$f_{Y|X}(Y|X=t) = \begin{cases} \dfrac{\beta^{\alpha}}{\Gamma(\alpha)}(Y-t)^{\alpha-1}e^{-\beta(Y-t)}, & y \geq t, \\ 0, & y < t. \end{cases} \tag{33}$$

Theorem 2: The ML estimation of the transmitted time X in the neuro-spike channel with an additive Gamma noise is obtained as

$$\hat{X}_{ML} = Y - \frac{\alpha-1}{\beta}. \tag{34}$$

Proof: The proof is given in Appendix B.

B. ML Detection

Similar to the AWGN channels which use signal constellations, we exploit discrete values for the input of the neuro-spike communication channel, i.e., the input spike train time intervals. Thus, for T-ary modulation, we can denote the transmission times by

$$X \in \{t_1, t_2, \ldots, t_T\}, \quad 0 \leq t_1 < t_2 < \ldots < t_T. \tag{35}$$

In the first step, by using discrete input times set, we analyze the error probability for binary modulation, where $T = 2$ with exploiting ML detection at the receiver. Let $X \in \{t_1, t_2\}, 0 \leq t_1 < t_2$, with $P_1 = \mathbb{P}(X = t_1)$ and $P_2 = \mathbb{P}(X = t_2)$. Hence, the log-likelihood ratio $L(Y)$ is obtained as

$$L(Y) = \log\left(\frac{f_{Y|X}(Y|X=t_2)}{f_{Y|X}(Y|X=t_1)}\right) = \Lambda(t_2) - \Lambda(t_1). \tag{36}$$

We can simplify $L(Y)$ as

$$L(Y) = \begin{cases} (\alpha-1)\ln\left(\dfrac{Y-t_2}{Y-t_1}\right) + \beta(t_2-t_1), & Y > t_2, \\ -\infty, & Y \leq t_2. \end{cases} \tag{37}$$

When $L(Y)$ is positive, t_2 has higher likelihood than t_1 and vice versa, when $L(Y)$ is negative t_2 has lower likelihood than t_1. When $L(Y) = 0$, there is no preference between t_1 and t_2. We relinquish this case, which happens with vanishing probability. Therefore, for ML detection, we set the decision threshold as $Y_{th} = 0$ and the decision rule is derived as

$$X_{ML} = \begin{cases} t_2, & L(Y) > 0, \\ t_1, & L(Y) < 0. \end{cases} \tag{38}$$

To consider maximum a posteriori (MAP) detection at the receiver, we exploit the same decision rule when we replace $L(Y) > 0$ with $L(Y) > \ln\left(\frac{P_1}{P_2}\right)$. Hence, for the MAP detection, we have

$$Y_{th} = L(Y) = \ln\left(\frac{P_1}{P_2}\right), \tag{39}$$

and the decision rule is derived as

$$X_{MAP} = \begin{cases} t_2, & L(Y) > \ln\left(\dfrac{P_1}{P_2}\right), \\ t_1, & L(Y) < \ln\left(\dfrac{P_1}{P_2}\right). \end{cases} \tag{40}$$

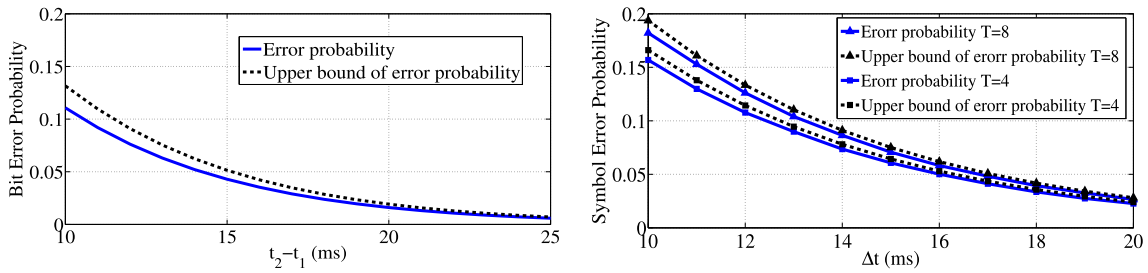

Fig. 6. (a) Bit error probability of binary modulation and its upper bound for $V_{th} = -55\,\text{mV}$ when $P_1 = 0.6$ and $P_2 = 0.4$. (b) Symbol error probability of T-ary modulation for different values of T which is obtained through Monte Carlo simulation and its upper bound for $V_{th} = -55\,\text{mV}$.

C. Error Probability Analysis for Binary Modulation

For binary modulation, the bit error probability is derived as

$$P_e = P_1 \times \mathbb{P}\{Y = t_2 | X = t_1\} + P_2 \times \mathbb{P}\{Y = t_1 | X = t_2\}, \tag{41}$$

where $\mathbb{P}\{Y = t_2 | X = t_1\}$ is the probability of $Y = t_2$ when $X = t_1$ and it can be obtained as

$$\mathbb{P}\{Y = t_2 | X = t_1\} = \int_{Y_{th}}^{\infty} f_{Y|X}\{Y | X = t_1\} dY. \tag{42}$$

It can be simplified as

$$\begin{aligned}\mathbb{P}\{Y = t_2 | X = t_1\} &= 1 - F_N(\alpha, \beta(Y_{th} - t_1)) \\ &= 1 - \frac{1}{\Gamma(\alpha)}\gamma(\alpha, \beta(Y_{th} - t_1)),\end{aligned} \tag{43}$$

where $F_N(\cdot)$ is CDF of channel jitter noise and Y_{th} is the decision threshold value of Y. Similarly, we have

$$\mathbb{P}\{Y = t_1 | X = t_2\} = \int_{t_2}^{Y_{th}} f_{Y|X}\{Y | X = t_2\} dY. \tag{44}$$

It can be simplified as

$$\begin{aligned}\mathbb{P}\{Y = t_1 | X = t_2\} &= F_N(\alpha, \beta(Y_{th} - t_2)) \\ &= \frac{1}{\Gamma(\alpha)}\gamma(\alpha, \beta(Y_{th} - t_2)),\end{aligned} \tag{45}$$

where $\mathbb{P}\{Y = t_1 | X = t_2\}$ is the probability of $Y = t_1$ when $X = t_2$. By inserting the expressions in (43) and (45) into (41), the bit error probability of binary modulation is derived as

$$P_e = P_1 - \frac{P_1}{\Gamma(\alpha)}\gamma(\alpha, \beta(Y_{th} - t_1)) + \frac{P_2}{\Gamma(\alpha)}\gamma(\alpha, \beta(Y_{th} - t_2)). \tag{46}$$

In the following, we derive an upper bound on the bit error probability of binary modulation when $P_1 \geq P_2$, which is simple to calculate and it closely approximates the exact error probability.

Theorem 3: Consider binary modulation with input spikes time intervals $X \in \{t_1, t_2\}$, $0 \leq t_1 < t_2$, with $\mathbb{P}(X = t_1) = P_1$, $\mathbb{P}(X = t_2) = P_2$ and $P_1 \geq P_2$. The upper bound on the bit error probability of neuro-spike channel with an additive Gamma noise by using the ML detector is obtained as

$$P_e < P_1 \left(1 - F_N(t_2 - t_1)\right). \tag{47}$$

Proof: The proof is given in Appendix C.

D. Symbol Error Probability of T-Ary Modulation

For T-ary modulation, we can easily generalize the symbol error probability bound. We assume input spikes time intervals $X \in \{t_1, t_2, \ldots, t_T\}$, where $0 \leq t_1 < t_2 < \ldots < t_T$ and $P_1 \geq P_2 \geq \ldots \geq P_T$, and thus, the upper bound on the symbol error probability is derived as

$$\begin{aligned}P_e &\leq \sum_{i=1}^{T-1} P_i \left(1 - F_N(t_{i+1} - t_i)\right) \\ &\leq \sum_{i=1}^{T-1} P_i \left(1 - \frac{1}{\Gamma(\alpha)}\gamma\left(\alpha, \beta(t_{i+1} - t_i)\right)\right).\end{aligned} \tag{48}$$

In a special case, when $P_1 = P_2 = \ldots = P_T$, we have

$$P_e \leq \frac{T-1}{T}\left(1 - \frac{1}{\Gamma(\alpha)}\gamma\left(\alpha, \beta\Delta t\right)\right), \tag{49}$$

where Δt is the average input spike train intervals.

E. Numerical Results

Fig. 6 (a) shows the bit error probability with binary modulation. This figure compares the exact value of the error probability and its upper bound. As can be observed, they are very close to each others. Fig. 6 (b) shows the symbol error probability with T-ary modulation for different values of T. This figure compares the error probability of this modulation which is obtained through Monte Carlo simulation and the upper bound of this error probability for $T = 4, 8$. It can be observed, the proposed upper bound is tight.

V. Conclusion

In this paper, we considered a neuro-spike communication system where information conveyed in the time intervals of input spike train. We have modeled this channel as an additive Gamma noise channel. We have indicated via numeral methods that the proposed channel model is suitable for a neuro-spike communication system exploiting temporal modulation.

Then, we have analyzed the channel capacity bounds versus different values of input spike train time intervals and the firing threshold of the receiver. It has been observed that the upper and lower bounds are close to each other for shorter input spikes intervals. According to the obtained results, we conclude that temporal coding has a higher efficiency than spike rate coding in terms of achievable data rate for the same spike frequencies. In addition, we have proposed optimum ML and MAP receivers and we have derived the bit error probability for ML receiver when the system uses binary modulation. Besides, we have obtained an upper bound for this error probability. Then, we have extended this upper bound to T-ary modulation. Simulation results have shown the upper bounds are tight for different modulations.

APPENDIX A
PROOF OF THEOREM 1

From (25), we have $I(X;Y) = h(Y) - h_{\mathbb{G}}(\alpha,\beta)$. Therefore, we can conclude that the $I(X;Y)$ achieves its maximum value via maximizing $h(Y)$ subject to the constraint $\mathbb{E}(X) \le m$ or equivalently $\mathbb{E}(Y) \le m + \frac{\alpha}{\beta}$. Hence, $I(X;Y)$ is maximized when $h(Y)$ gets its maximum value subject to $f_Y(y) = 0,\ y < 0$, and $\mathbb{E}(Y) \le m + \frac{\alpha}{\beta}$. To derive the upper bound of the neuro-spike communication channel with an additive Gamma noise, we consider an exponential distribution for the output spikes time intervals which is defined over the interval $(0,\infty)$, since the exponential distribution is known as the entropy maximizing distribution when a random variable has a mean constraint [49]. By assuming $Y \sim \exp(\frac{1}{m+\frac{\alpha}{\beta}})$; it is obtained that $h(Y) = \ln\left((m+\frac{\alpha}{\beta})e\right)$ and $h(Y)$ has the maximum value for any possible distributions of Y with $\mathbb{E}(Y) \le m + \frac{\alpha}{\beta}$. Hence, we have

$$C \le \ln\left((m+\frac{\alpha}{\beta})e\right) - (\alpha - \ln(\beta) + \ln(\Gamma(\alpha)) + (1-\alpha)\Psi(\alpha)), \quad \text{(A.1)}$$

that it can be simplified as

$$C \le \ln\left(\frac{(m\beta+\alpha)e}{\Gamma(\alpha)}\right) - \alpha - (1-\alpha)\Psi(\alpha) = C_{\text{Upper}}. \quad \text{(A.2)}$$

To derive the lower bound of the neuro-spike communication channel with an additive Gamma noise, we consider the input spike train time intervals, i.e., X is Gamma distributed with α' and β parameters. Hence, when the input distribution is assumed as $\mathbb{G}(m\beta,\beta)$ since $\mathbb{E}(X) = m$, then according to Property 2, the output distribution is obtained as $Y \sim \mathbb{G}(\alpha + m\beta,\beta)$. Therefore, we have $h(Y) = h_{\mathbb{G}}(\alpha+m\beta,\beta)$. By using Property 1, we derive

$$C \ge m\beta + \ln\left(\frac{\ln(\alpha+m\beta)}{\ln(\alpha)}\right) + (1-\alpha-m\beta)\Psi(\alpha+m\beta) - (1-\alpha)\Psi(\alpha) = C_{\text{Lower}}. \quad \text{(A.3)}$$

Note that in this case $f_Y(y)$ is not necessarily an entropy maximizing distribution for a given mean of $m + \frac{\alpha}{\beta}$. Thus, we have $C_{\text{Lower}} \le C \le C_{\text{Upper}}$.

APPENDIX B
PROOF OF THEOREM 2

We denote the log-likelihood function as $\Lambda(t_i) = \ln(f_{Y|X}(Y|X=t_i))$. Since $\ln(x)$ is a monotonic function, we have

$$\hat{X}_{ML} = \arg\max_{t_i} f_{Y|X}(Y|X=t_i) = \arg\max_{t_i} \Lambda(t_i), \quad \text{(B.1)}$$

where

$$\Lambda(t_i) = \begin{cases} \alpha\ln(\beta) - \ln(\Gamma(\alpha)) \\ +(\alpha-1)\ln(Y-t_i) \\ -\beta(Y-t_i), & Y > t_i, \\ -\infty, & Y \le t_i. \end{cases} \quad \text{(B.2)}$$

By solving $\frac{\delta\Lambda(t_i)}{\delta t_i} = 0$ over values of $Y > t_i$, we derive the MLE as (34).

APPENDIX C
PROOF OF THEOREM 3

To prove (47), let

$$\eta = \int_{t_2}^{\infty} f_{Y|X}(Y|X=t_1)dY - \int_{Y_{th}}^{\infty} f_{Y|X}(Y|X=t_1)dY = \int_{t_2}^{Y_{th}} f_{Y|X}(Y|X=t_1)dY. \quad \text{(C.1)}$$

Since $Y_{th} > t_2$, we have $\eta > 0$. Moreover, we can write

$$\mathbb{P}\{Y=t_2|X=t_1\} = \int_{Y_{th}}^{\infty} f_{Y|X}(Y|X=t_1)dY = \int_{t_2}^{\infty} f_{Y|X}(Y|X=t_1)dY - \eta. \quad \text{(C.2)}$$

Based on the ML detection, when $Y \le Y_{th}$, it can be concluded that $f_{Y|X}(Y|X=t_1) \le f_{Y|X}(Y|X=t_2)$. Thus, we have

$$\mathbb{P}\{Y=t_1|X=t_2\} = \int_{t_2}^{Y_{th}} f_{Y|X}(Y|X=t_2)dY \le \int_{t_2}^{Y_{th}} f_{Y|X}(Y|X=t_1)dY = \eta. \quad \text{(C.3)}$$

Finally, based on the expressions in (C.1) and (C.3), we can write

$$\begin{aligned} P_e &= P_1\,\mathbb{P}\{Y=t_2|X=t_1\} + P_2\,\mathbb{P}\{Y=t_1|X=t_2\} \\ &\le P_1\left(\int_{t_2}^{\infty} f_{Y|X}(Y|X)dY - \eta\right) + P_2\eta \\ &= P_1\int_{t_2}^{\infty} f_{Y|X}(Y|X=t_1)dY - (P_1-P_2)\eta. \end{aligned} \quad \text{(C.4)}$$

Since we assume $P_1 \geq P_2$, we conclude $(P_1 - P_2)\eta \geq 0$. Hence, we have

$$P_e \leq P_1 \int_{t_2}^{\infty} f_{Y|X}(Y|X = t_1)dY. \tag{C.5}$$

According to the definition of CDF function, we can write $\int_{t_2}^{\infty} f_{Y|X}(Y|X = t_1)dY = 1 - F_N(t_2 - t_1)$. Hence, the expression in (47) becomes.

REFERENCES

[1] K. Aghababaiyan, V. Shah-Mansouri, and B. Maham, "Capacity bounds of neuro-spike communication by exploiting temporal modulations," in *Proc. IEEE Wireless Commun. Netw. Conf. (WCNC)*, Barcelona, Spain, Apr. 2018.

[2] I. F. Akyildiz, J. M. Jornet, and M. Pierobon, "Nanonetworks: A new frontier in communications," *Commun. ACM*, vol. 54, no. 11, pp. 84–89, Nov. 2011.

[3] J. M. Jornet and I. F. Akyildiz, "Graphene-based plasmonic nano–antenna for terahertz band communication in nanonetworks," *IEEE J. Sel. Areas Commun.*, vol. 31, no. 12, pp. 685–694, Dec. 2013.

[4] D. Malak and O. B. Akan, "Molecular communication nanonetworks inside human body," *Nano Commun. Netw.*, vol. 3, no. 1, pp. 19–35, Mar. 2012.

[5] G. E. Santagati and T. Melodia, "Opto-ultrasonic communications in wireless body area nanonetworks," *Asilomar Conf. Signals, Syst. Comput.*, Pacific Grove, CA, USA, Nov. 2013.

[6] S. Balasubramaniam *et al.*, "Development of artificial neuronal networks for molecular communication," *Nano Commun. Netw.*, vol. 2, no. 2, pp. 150–160, Sep. 2011.

[7] D. Seo, J. M. Carmena, J. M. Rabaey, E. Alon, and M. M. Maharbiz, "Neural dust: An ultrasonic, low power solution for chronic brain-machine interfaces," Jul. 2013, *arXiv:1307.2196*, [Online]. Available: https://arxiv.org/abs/1307.2196

[8] J. Suzuki, S. Balasubramaniam, S. Pautot, V. D. P. Meza, and Y. Koucheryavy, "A service-oriented architecture for body area nanonetworks with neuron-based molecular communication," *Mobile Netw. Appl.*, vol. 19, no. 6, pp. 707–717, Dec. 2014.

[9] F. Mesiti and I. Balasingham, "Nanomachine-to-neuron communication interfaces for neuronal stimulation at nanoscale," *IEEE J. Sel. Areas Commun.*, vol. 31, no. 12, pp. 695–704, Dec. 2013.

[10] F. Mesiti and I. Balasingham, "Novel treatment strategies for neurodegenerative diseases based on RF exposure," in *Proc. 4th Int. Symp. Appl. Sci. Biomed. Commun. Technol.*, Barcelona, Spain, Oct. 2011, Art. no. 100.

[11] P. Greengard, "The neurobiology of slow synaptic transmission," *Science*, vol. 294, no. 5544, pp. 1024–1030, Nov. 2001.

[12] P. Dayan and L. F. Abbott, *Theoretical Neuroscience*, vol. 806. Cambridge, MA, USA: MIT Press, 2001.

[13] S. E. Fienberg, "Stochastic models for single neuron firing trains: A survey," *Adv. Appl. Probab.*, vol. 7, no. 2, pp. 259–260, Jun. 1975.

[14] A. A. Faisal, L. P. J. Selen, and D. M. Wolpert, "Noise in the nervous system," *Nature Rev. Neurosci.*, vol. 9, no. 4, pp. 292–303, 2008.

[15] R. B. Stein, "A theoretical analysis of neuronal variability," *Biophys. J.*, vol. 5, no. 2, pp. 173–194, Mar. 1965.

[16] D. Malak and O. B. Akan, "A communication theoretical analysis of synaptic multiple–access channel in hippocampal–cortical neurons," *IEEE Trans. Commun.*, vol. 61, no. 6, pp. 2457–2467, Jun. 2013.

[17] E. Balevi and O. B. Akan, "A physical channel model for nanoscale neuro–spike communications," *IEEE Trans. Commun.*, vol. 61, no. 3, pp. 1178–1187, Mar. 2013.

[18] J. Delcastillo and E. Suckling, "Possible quantal nature of subthreshold responses at single nodes of ranvier," *Fed. Proc.*, vol. 16, no. 1, p. 29, Jan. 1957.

[19] Y. Lass and M. Abeles, "Transmission of information by the axon: Noise and memory in the myelinated nerve fiber of the frog," *Biol. Cybern.*, vol. 19, no. 2, pp. 61–67, Jun. 1975.

[20] T. Berger and W. B. Levy, "A mathematical theory of energy efficient neural computation and communication," *IEEE Trans. Inf. Theory*, vol. 56, no. 2, pp. 852–874, Feb. 2010.

[21] M. Veletic, P. A. Floor, Z. Babic, and I. Balasingham, "Peer-to-peer communication in neuronal nano–network," *IEEE Trans. Commun.*, vol. 64, no. 3, pp. 1153–1166, Mar. 2016.

[22] T. Khan, B. A. Bilgin, and O. B. Akan, "Diffusion–based model for synaptic molecular communication channel," *IEEE Trans. Nanobiosci.*, vol. 16, no. 4, pp. 299–308, Jun. 2017.

[23] H. Ramezani and O. B. Akan, "Information capacity of vesicle release in neuro–spike communication," *IEEE Commun. Lett.*, vol. 22, no. 1, pp. 41–44, Jan. 2018.

[24] M. Veletic, P. A. Floor, Y. Chahibi, and I. Balasingham, "On the upper bound of the information capacity in neuronal synapses," *IEEE Trans. Commun.*, vol. 64, no. 12, pp. 5025–5036, Dec. 2016.

[25] K. Aghababaiyan, V. Shah-Mansouri, and B. Maham, "Axonal channel capacity in neuro–spike communication," *IEEE Trans. Nanobiosci.*, vol. 17, no. 1, pp. 78–87, Jan. 2018.

[26] K. Aghababaiyan and B. Maham, "Axonal transmission analysis in neuro-spike communication," in *Proc. IEEE Int. Conf. Commun. (ICC)*, Paris, France, May 2017.

[27] M. Pierobon and I. F. Akyildiz, "A physical end-to-end model for molecular communication in nanonetworks," *IEEE J. Sel. Areas Commun.*, vol. 28, no. 4, pp. 602–611, May 2010.

[28] K. Aghababaiyan, V. Shah-Mansouri, and B. Maham, "Joint optimization of input spike rate and receiver decision threshold to maximize achievable bit rate of neuro–spike communication channel," *IEEE Trans. Nanobiosci.*, vol. 18, no. 2, pp. 117–127, Apr. 2019.

[29] K. Aghababaiyan and B. Maham, "Error probability analysis of neuro-spike communication channel," in *Proc. IEEE Symp. Comput. Commun. (ISCC)*, Heraklion, Greece, Jul. 2017.

[30] N. Hatsopoulos, S. Geman, A. Amarasingham, and E. Bienenstock, "At what time scale does the nervous system operate?" *Neurocomputing*, vols. 52–54, pp. 25–29, Jun. 2003.

[31] C. Stam, B. Jones, G. Nolte, M. Breakspear, and P. Scheltens, "Small–world networks and functional connectivity in Alzheimer's disease," *Cerebral Cortex*, vol. 17, no. 1, pp. 92–99, Feb. 2006.

[32] N. Rouach *et al.*, "Gap junctions and connexin expression in the normal and pathological central nervous system," *Biol. Cell*, vol. 94, nos. 7–8, pp. 457–475, Nov. 2002.

[33] N. Li, T.-W. Chen, Z. V. Guo, C. R. Gerfen, and K. Svoboda, "A motor cortex circuit for motor planning and movement," *Nature*, vol. 519, no. 7541, pp. 51–56, Mar. 2015.

[34] J. V. Trontelj, M. Mihelin, J. M. Fernandez, and E. Stalberg, "Axonal stimulation for end-plate jitter studies.," *J. Neurol., Neurosurgery Psychiatry*, vol. 49, no. 6, pp. 677–685, Jun. 1986.

[35] O. A. C. Petroff, "Book review: GABA and glutamate in the human brain," *Neuroscientist*, vol. 8, no. 6, pp. 562–573, Dec. 2002.

[36] I. Karatzas and S. E. Shreve, "Brownian motion," in *Brownian Motion and Stochastic Calculus*. New York, NY, USA: Springer, 1998, pp. 47–127.

[37] E. L. Cussler, *Diffusion: Mass Transfer in Fluid Systems*. Cambridge, U.K.: Cambridge Univ. Press, 2009.

[38] E. P. Huang, "Synaptic transmission: Spillover at central synapses," *Current Biol.*, vol. 8, no. 17, pp. R613–R615, Aug. 1998.

[39] E. Stone, K. Hoffman, and M. Kavanaugh, "Identifying neurotransmitter spill-over in hippocampal field recordings," *Math. Biosciences*, vol. 240, no. 2, pp. 169–186, Dec. 2012.

[40] A. N. Burkitt, "A review of the integrate-and-fire neuron model: I. Homogeneous synaptic input," *Biological*, vol. 95, no. 1, pp. 1–19, Jul. 2006.

[41] J. Ruppersberg, E. V. Kitzing, and R. Schoepfer, "The mechanism of magnesium block of NMDA receptors," *Seminars Neurosci.*, vol. 6, no. 2, pp. 87–96, Apr. 1994.

[42] D. A. Rusakov, L. P. Savtchenko, K. Zheng, and J. M. Henley, "Shaping the synaptic signal: Molecular mobility inside and outside the cleft," *Trends Neurosci.*, vol. 34, no. 7, pp. 359–369, Jul. 2011.

[43] M. L. Dustin and D. R. Colman, "Neural and immunological synaptic relations," *Science*, vol. 298, no. 5594, pp. 785–789, Oct. 2002.

[44] T. A. Nielsen, D. A. DiGregorio, and R. A. Silver, "Modulation of glutamate mobility reveals the mechanism underlying slow-rising AMPAR EPSCs and the diffusion coefficient in the synaptic cleft," *Neuron*, vol. 42, no. 5, pp. 757–771, Jun. 2004.

[45] J. Montes, J. M. Peña, J. Defelipe, O. Herreras, and A. Merchan-Perez, "The influence of synaptic size on AMPA receptor activation: A Monte Carlo model," *PLoS ONE*, vol. 10, no. 6, Jun. 2015, Art. no. e0130924.

[46] A. Manwani and C. Koch, "Detecting and estimating signals over noisy and unreliable synapses: Information–theoretic analysis," *Neural Comput.*, vol. 13, no. 1, pp. 1–33, Jan. 2001.
[47] D. A. Turner, "Waveform and amplitude characteristics of evoked responses to dendritic stimulation of CA1 guinea-pig pyramidal cells.," *The J. Physiol.*, vol. 395, no. 1, pp. 419–439, Jan. 1988.
[48] A. Borst and F. E. Theunissen, "Information theory and neural coding," *Nat. Neurosci.*, vol. 2, no. 11, pp. 947–957, Nov. 1999.
[49] T. M. Cover and J. A. Thomas, *Elements of Information Theory*. Hoboken, NJ, USA: Wiley, 2012.

Keyvan Aghababaiyan received the B.Sc. degree (Hons.) in electrical engineering from the Amirkabir University of Technology, Tehran, Iran, in 2011, the M.Sc. degree in electrical engineering from the Sharif University of Technology, Tehran, in 2013, and the Ph.D. degree from the University of Tehran, in 2019. He is currently a Postdoctoral Researcher with the School of Electrical and Computer Engineering, University of Tehran. His research interests include Nano-neural communication systems, molecular communication, wireless communication, and direction of arrival estimation.

Vahid Shah-Mansouri (Member, IEEE) received the B.Sc. degree and in electrical engineering from the University of Tehran, in 2003, the M.Sc. degree in electrical engineering from the Sharif University of Technology, in 2005, and Ph.D. degrees in electrical engineering from the University of British Columbia, in 2011. Since 2013, he has been an Assistant Professor with the Department of Electrical and Computer Engineering, University of Tehran, Iran. His research interests include the design and mathematical modeling of communication and computer networks, heterogeneous networks, 5G core architecture, and Nano-neural communication systems.

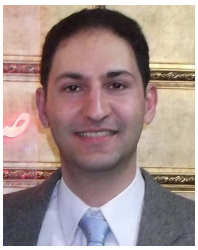

Behrouz Maham (Senior Member, IEEE) received the B.Sc. and M.Sc. degrees in electrical engineering from the University of Tehran, Iran, in 2005 and 2007, respectively, and the Ph.D. degree from the University of Oslo, Norway, in 2010. From September 2008 to August 2009, he was with the Department of Electrical Engineering, Stanford University, USA. He was a Faculty Member with the School of ECE, University of Tehran, from September 2011 to September 2015. He is currently an Assistant Professor with the School of Engineering, Nazarbayev University. He is affiliated with TWAS. He has more than 120 publications in major technical journals and conferences. His fields of interest include wireless communication and networking and Nano-neural communication systems.